

Clustering Analysis of Periodic Point Vortices with the *L* Function

MAKOTO UMEKI*

*Department of Physics, Graduate School of Science, University of Tokyo,
7-3-1 Hongo, Bunkyo-ku, Tokyo, 113-0033 Japan*

A motion of point vortices with periodic boundary conditions is studied by using Weierstrass zeta functions. Scattering and recoupling of a vortex pair by a third vortex becomes remarkable when the vortex density is large. Clustering of vortices with various initial conditions is quantitated by the *L* function used in point process theory in spatial ecology. It is shown that clustering persists if it is initially clustered like an infinite row or a checkered pattern.

KEYWORDS: point vortex, two-dimensional turbulence, Mathematica, *L* function, point process theory

A statistical approach to a problem of assemblies of point vortices (PVs) goes back to Onsager (1949). A state of negative temperature is considered to be related to clustering of vortices rotating in the same direction and the inverse energy cascade predicted in the two-dimensional Navier-Stokes (2D NS) turbulence. In many numerical simulations, PVs are bounded in a circular wall, since a velocity field due to a PV can be computed by including a single mirror image. Although the axisymmetry with respect to the origin is conserved, the spatial homogeneity is not guaranteed in such a circular system. There has been a numerical difficulty in a simulation of vortices in a box that there emerges an infinite sequence of virtual images. Our objective is to study turbulent motions and clustering of many PVs in a periodic box using Weierstrass zeta functions.

Let us start by representing the 2D NS equation in terms of a complex position $z = x + iy$, velocity $q = u - iv$, pressure p and the kinematic viscosity ν as

$$q_t + qq_{\bar{z}} + \bar{q}q_z = -2p_z + 4\nu q_{z\bar{z}}. \quad (1)$$

Here, \bar{q} denotes the complex conjugate of q and we use the relations $\partial_x = \partial_z + \partial_{\bar{z}}$, $\partial_y = i(\partial_z - \partial_{\bar{z}})$, $u = (q + \bar{q})/2$, $v = i(q - \bar{q})/2$ and $\Delta = 4\partial_{z\bar{z}}$. The incompressible condition gives $\nabla \cdot \mathbf{v} = \bar{q}_z + q_{\bar{z}} = 0$. The vorticity $\omega = v_x - u_y$ can be expressed by q as $\omega = 2iq_{\bar{z}}$.

If the flow is irrotational $\omega = 0$, then $q_{\bar{z}} = 0$, q depends on only z (and t) and theory of conformal mapping can be applied. Equations for the vorticity and pressure are respectively

$$q_{zt} + qq_{\bar{z}\bar{z}} + \bar{q}q_{z\bar{z}} = 4\nu q_{z\bar{z}\bar{z}}, \quad (2)$$

and $p_{z\bar{z}} = -(q_z\bar{q}_{\bar{z}} + \bar{q}_zq_{\bar{z}})/2$.

According to Tkachenko,^{1,2} the velocity field due to a single PV at the origin with periodic boundary conditions (BCs) is equivalent to that due to PVs on the lattice $z_{mn} = 2m\omega_1 + 2n\omega_2$, where the complex numbers ω_1, ω_2 are the half periods of the lattice and m, n are arbitrary integers. The ratio of two periods $\tau = \omega_1/\omega_2$ can be restricted in the region

$$\text{Im}\tau > 0, \quad |\text{Re}\tau| < 1/2, \quad |\tau| \geq 1. \quad (3)$$

We concentrate on the case of square periodic BCs,

which is usually adapted for numerical studies of the two-dimensional turbulence by a choice of $\tau = i$. However, we can deal with an arbitrary periodic parallelogram by considering various values of τ satisfying the condition (3).

The velocity field due to a PV of strength $\kappa = 2\pi$ is given by the Weierstrass zeta function $\zeta(z; \omega_1, \omega_2)$ along with a rigid rotation term as follows:

$$\bar{q} = i\overline{\zeta(z)} - i\Omega z \equiv w(z). \quad (4)$$

Since the vortex lattice undergoes rigid rotation with angular velocity Ω given by $\Omega = \pi/[4\text{Im}(\bar{\omega}_1\omega_2)]$, the second term in Eq.(4) is necessary in order to cancel the velocity circulation on the boundary. The vortex density $n = 1/[4\text{Im}(\bar{\omega}_1\omega_2)]$, the angular velocity Ω and the vortex strength κ are related as $\kappa n = 2\Omega$. If the length of the side of the square is unit, then $\omega_1 = 1/2$, $\omega_2 = i/2$, $\Omega = \pi$ and the vortex strength κ becomes 2π .

The equation for the streamline $\psi = \text{const.}$, where ψ is the streamfunction, is equivalent to $dx/\psi_y = -dy/\psi_x$. Using the relations $u = \psi_y$ and $v = -\psi_x$, ψ is expressed as $\psi = \int u dy + f(x)$. The sigma and zeta functions of Weierstrass are related as $\zeta(z) = \sigma'(z)/\sigma(z)$. This relation is consistent with the asymptotic forms $\zeta \sim 1/z$ and $\sigma \sim z$ when $z \sim 0$. Using the above results, ψ for a single vortex lattice centered at the origin is given by

$$\psi = -\text{Re} \ln \sigma(z) + \Omega|z|^2/2. \quad (5)$$

There is a minimum of ψ in the periodic case, in contrast with the unbounded plane giving no limits on ψ .

For an assembly of PVs, we consider the case $\kappa_i = 2\pi\mu_i$, $\mu_i = 1, i = 1, \dots, N_1$ and $\mu_i = -1, i = N_1 + 1, \dots, N (= N_1 + N_2)$ for simplicity. Therefore, ψ for N PVs located at z_i is given by

$$\psi = \sum_{i=1}^N \mu_i \{ -\text{Re}[\ln \sigma(z - z_i)] + \Omega|z - z_i|^2/2 \}. \quad (6)$$

Using Eq. (4), the equation of motion of PVs with square periodic BCs can be expressed as³

$$\dot{z}_i = \sum_{j \neq i} \mu_j w(z_i - z_j). \quad (7)$$

The equation can be rewritten in Hamiltonian form as $\mu_i dz_i/dt = \partial H/\partial \bar{z}_i$, where the Hamiltonian H can be expressed as $H = \sum_{i=1}^N \mu_i h_i = \sum_{i=1}^N \sum_{j=i+1}^N \mu_i \mu_j h_{ij}$, $h_{ij} = -\text{Re}[\ln \sigma(z_i - z_j)] + \Omega|z_i - z_j|^2/2$. The Hamiltonian,

*E-mail address: umeki@phys.s.u-tokyo.ac.jp

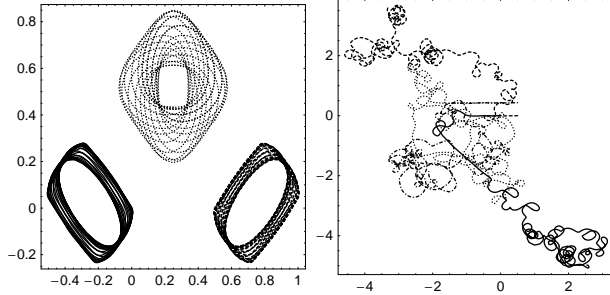


Fig. 1. Trajectories of three (a) and four (b). PVs 1, 2, 3 and 4 are denoted by a solid, dashed, dotted and dotted-dashed curve, respectively.

which is a total kinetic energy minus self induced kinetic energy of PVs, can be interpreted as a sum of kinetic energy due to an interaction between pairs of PVs.

If *Mathematica* is used, we can compute the Weierstrass zeta function as we use the sinusoidal function in a Fortran code. The system (4,7) is solved numerically by the *NDSolve* of *Mathematica* 5.2 installed in the PC having an AMD Athlon 64x2 3800 CPU, 2GB memory and Windows XP OS. The computation is realistic since the CPU time in such a PC environment is between two and five days for 100 PVs and 10 eddy turnover times.

If PVs lie in an unbounded domain, the system has four integrals,⁴ the Hamiltonian $H_u = -\sum \mu_i \mu_j \ln |z_i - z_j|$, two components of the linear impulse $\mathbf{I} = (I_x, I_y)$, $I_x = \sum \mu_i \text{Re}[z_i]$, $I_y = \sum \mu_i \text{Im}[z_i]$, and the angular impulse $A = \sum \mu_i |z_i|^2$. Since the system in a periodic box has no circular symmetry, A is no more constant, but H , I_x , and I_y remains to be conserved. Since there are three conserved quantities, the system of three PVs is integrable, while the four PVs show chaos.

Examples of trajectories of three PVs $\mu_i = (2, 2, -1)$ with an initial condition $(z_1, z_2, z_3) = (0, 0.5, 0.25 + i\sqrt{3}/4)$ located at the vertices of a triangular, and of four PVs $\mu_i = (2, 2, -1, -1)$ and $(z_1, z_2, z_3, z_4) = (0, 0.5, i\sqrt{3}/4, 0.5 + i\sqrt{3}/4)$ at $t = 0$ located as a square, are given in Figure 1a and 1b, respectively. The first case leads to collapse if the PVs are in an unbounded plane.

To analyze the spatial distribution of many PVs, we introduce the L function used in point process theory in spatial ecology.^{5,6} Let $\vec{x}_i = (x_i, y_i)$ be the position of N points randomly distributed in an area S . The K function is defined by

$$K(r) = (\lambda N)^{-1} \sum_{i=1}^N \sum_{j=1, j \neq i}^N \theta(|\vec{x}_i - \vec{x}_j| \leq r), \quad (8)$$

where $\lambda = N/S$ is the number density of the points and $\theta(x)$ is the step function. An extra function added in (8) in order to modify to the edge effect is unnecessary in the present periodic case.

If the distribution of points obeys completely spatially randomness (CSR) which is synonymous with a homogeneous Poisson process, $K(r)$ becomes the area of the circle with radius r ; i.e. $K(r) = \pi r^2$. Then, it is convenient to introduce the L function as

$$L(r) = \sqrt{K(r)/\pi} - r. \quad (9)$$

CSR gives $L = 0$. For clustering, i.e. points like to stay close to the other point, we have $L > 0$. If points like to be spaced with each other, $L < 0$.

Following Novikov (1976)⁷ in an unbounded plane, we have a relation between the distance r_{jl} of two PVs of strength κ_j and κ_l and the energy spectrum $E(k)$ as

$$E(k) = (4\pi k)^{-1} [\sum_j \kappa_j^2 + 2 \sum_{j < l} \kappa_j \kappa_l J_0(kr_{jl})]. \quad (10)$$

If $\kappa_j = \kappa$ for all j , we have

$$E(k) = \kappa^2 (4\pi k)^{-1} [N + 2 \sum_{j < l} J_0(kr_{jl})], \quad (11)$$

and using the number density $\rho(r)$ at the distance r between two PVs, we have in the continuous limit $E(k) = E_1(k) + E_2(k)$, where $E_1(k) = \kappa^2 N / 4\pi k$ and $E_2(k) = \kappa^2 / 2\pi k \int_0^\infty J_0(kr) \rho(r) dr$. $E_1(k)$ and $E_2(k)$ correspond to the self energy of each vortex and interaction energy between two PVs, similarly to h_{ij} . We have a relation between the $K(r)$ and $\rho(r)$ as $K(r) = l^2 / N' \int_0^r \rho(r') dr'$, where $\rho(r)$ is normalized by the upper limit l of r and the total number $N' = N(N-1)/2$ of pairs of PVs.

If $\rho(r) = Cr^\alpha$, we can integrate $E_2(k)$ into $E_2(k) = \kappa^2 C k^{-\alpha-2} \Gamma((\alpha+1)/2) / 2\pi \Gamma((1-\alpha)/2)$, for $-1 < \alpha < 1/2$. The value $\alpha = -1/3$ gives the Kolmogorov spectrum $k^{-5/3}$ in 3D turbulence.

Formally the CSR value $\alpha = 1$ in two dimensions gives the k^{-3} spectrum, although the integral does not converge. In order to avoid the divergence, the exponential decay in $\rho(r)$ may be introduced. Otherwise, we may put the upper limit l in the range of integration in $E_2(k)$. Using the normalization $r = lr'$ and the integral expressed by a regularized hypergeometric function as $\int_0^1 J_0(kr) r^\alpha dr = \Gamma((1+\alpha)/2) {}_1F_2((1+\alpha)/2; \{1, (3+\alpha)/2\}; -k^2/4) / 2\Gamma((3+\alpha)/2)$, for $\alpha > -1$, $E_2(k)$ is written as $E_2(k) = \kappa^2 C l^{\alpha+1} \Gamma((1+\alpha)/2) {}_1F_2((1+\alpha)/2; \{1, (3+\alpha)/2\}; -(kl)^2/4) / 4\pi k \Gamma((3+\alpha)/2)$.

If we use the CSR distribution $\rho(r) = \pi N' l^{-2} r$, we have $\int_0^1 J_0(kr) r dr = J_1(k)/k$. Then $E_2(k)$ is given by

$$E_2(k) = \kappa^2 N' l^{-1} k^{-2} J_1(k)/2. \quad (12)$$

For large kl , we have the asymptotic form

$$E_2(k) \simeq \sqrt{1/2\pi} \kappa^2 N' l (kl)^{-5/2} \cos(kl - 3\pi/4). \quad (13)$$

The value of $E_2(k)$ is oscillatory as k increases with the amplitude decaying as $k^{-5/2}$. The total energy spectrum of course does not become negative because of $E_1(k) \gg E_2(k)$ for large k .

For numerical study, we first consider the assembly of PVs having the same positive strength. The following four typical cases are considered; Case (I) an infinite row which is a discrete model of the vortex sheet, Case (II) PVs located randomly in checkered patterns (*Ichimatsu moyo* in Japanese), Case (III) PVs located randomly in the 10×10 subsquares, and Case (IV) CSR in the unit square. Here, the word *CSR* implies that PVs are distributed by random numbers generated by a single run. The initial conditions, the number N of PVs, the final time t_f and the values of three conserved quantities are summarized in Table 1. The relative precision of H in the numerical simulation is confirmed to be less than $10^{-6} \sim 10^{-5}$ up to $t = t_f$. Figure 2 shows initial and

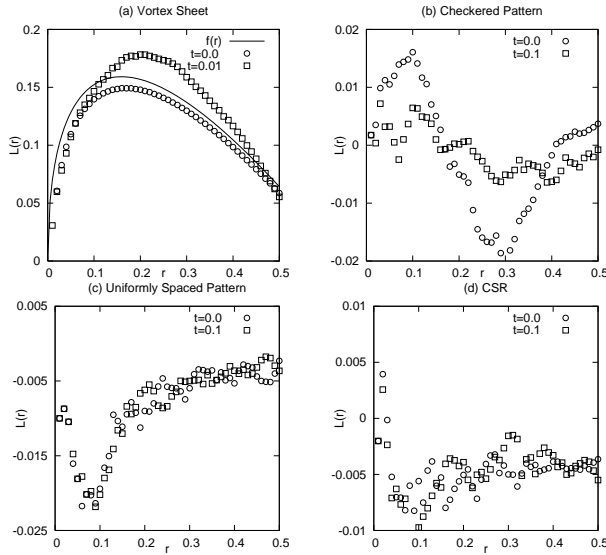


Fig. 2. The L functions. (a) corresponds to (I), (b) to (II), (c) to (III) and (d) to (IV)

final distributions of PVs and the L function.

For Case (I), PVs of the same strength 2π are located initially on x -axis as $z_j(0) = j/N + \epsilon \sin 2\pi j/N$, $j = 1, \dots, N$, where $\epsilon = 0.05$. If ϵ is fixed and N is increased, pairing of two adjacent PVs becomes more conspicuous than the winding of the sheet due to the Kelvin-Helmholtz instability. The growth rate $\sigma = \kappa\pi p(1-p)/a^2$ of the pairing instability in an unbounded plane takes a maximum at $p = 1/2$, where a is the distance of two adjacent PVs.⁴ The modulus 1 is suitably taken so that PVs are plotted in the square chosen in the following figures. Of course, PVs wander chaotically from one square to another.

For $\epsilon = 0$, we have $\rho(r) = 2N'l^{-2}$, $K(r) = 2r$ and the average Hamiltonian $\langle h \rangle = 2 \sum_{i>j} h_{ij}/N(N-1) = 2[\sum_{j=1}^{N/2-1} \psi(j/N) + \psi(1/2)/2]/N(N-1) \sim 2 \int_0^{1/2} dx \psi(x)$. Since $\psi(x) \sim -\ln|x|$ for $x \sim 0$, $\langle h \rangle \equiv \int_S dx dy \psi(z) \rho(z)$ gives a finite value for $\rho = Cr^\alpha$, $r \sim 0$, and $\alpha > -2$. Since $\alpha < 1$ corresponds to clustering, clustering with $\alpha < -2$ cannot occur from the initial condition with a finite $\langle h \rangle$.

Second, we consider Case (II) where the initial PVs are located randomly in eight segments showing a checkered pattern. $L(r) > 0$ for $0 < r < 0.15$ implies that the PVs are clustered, while $L(r) < 0$ for $0.15 < r < 0.4$ means that PVs are uniformly spaced at larger scales. We observe that this tendency remains at $t = t_f$ although it becomes somewhat weak and has an additional oscillatory behavior.

Third, Case (III) has uniformly spaced PVs initially. $L(r)$ has a large negative value for all r . We observe that $L(r)$ is almost the same during $t \in [0, t_f]$.

Fourth, we examine the completely spatially random

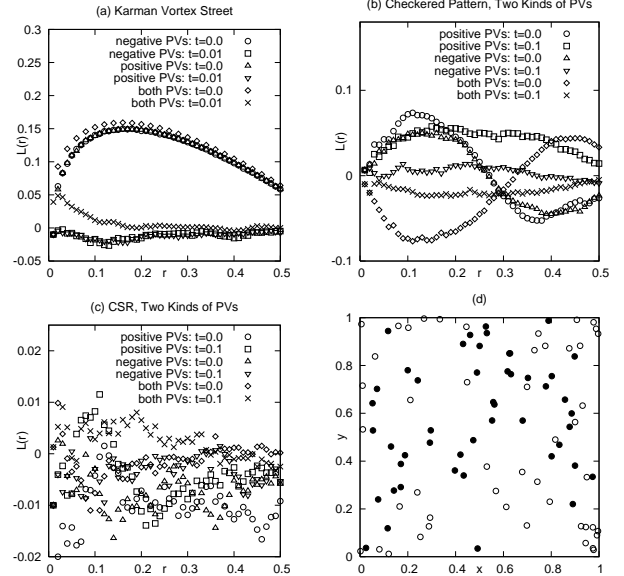


Fig. 3. The L functions. (a) to (V), (b) to (VI) and (c) to (VII). (d) shows the distribution of PVs for (VI) at $t = 0.1$. White (black) circles denote positive (negative) PVs.

distribution of PVs at $t = 0$ in Case (IV). We observe slightly negative values of $L(r)$ at $t = 0$ and t_f , but we do not see any significant difference between initial and final distributions.

Next, we consider the system with both positive and negative PVs of the same strength and the same numbers. The following three typical cases are examined; Case (V) Kármán vortex street, Case (VI) positive and negative PVs are located alternatively in checkered segments (16 subsquares), and Case (V) completely spatially random distribution. The initial conditions, the number N_1, N_2 of PVs, the final time t_f and the values of three conserved quantities are summarized in Table 2.

First, we consider Case (V) given by the following expression: $\mu_j = (-1, 1)$, $z_j(0) = (j/N_1 + \epsilon(R+iR), j/N_2 + 1/N + ih + \epsilon(R+iR))$ for $j = (1, \dots, N_1, N_1 + 1, \dots, N)$, where $\epsilon = 10^{-4}$, R denotes random numbers and the distance h between two rows is taken as $1/N$. Only in this case, negative PVs are first numbered. At about $t = 0.001$ we observe that the two rows begin to break with the paring instability.⁴

For the two kinds of PVs, we introduce $K_{lm}(r)$ for $(l, m) = (+, +), (-, -)$ and $(+, -)$ as

$$K_{lm}(r) = (\lambda N)^{-1} \sum_i \sum_j \theta(|\vec{x}_i - \vec{x}_j| \leq r), \quad (14)$$

where the sum is for $i, j = 1 \dots, N_1$ except for $j = i$ if $(l, m) = (+, +)$. The case $(l, m) = (-, -)$ is similar. The sum for $(l, m) = (+, -)$ is both $i = 1 \dots, N_1$, $j = N_1 + 1 \dots, N_2$ and $i = N_1 + 1 \dots, N_2$, $j = 1 \dots, N_1$. We define $L_{lm}(r)$ from $K_{lm}(r)$ similarly to Eq. (9). We observe strong clustering for $(l, m) = (+, -)$ at $t = 0.01$ corresponding to the pairing instability.

Second, for Case (VI), we observe the anisotropy, i.e., $L_{++}(r) \gg L_{--}(r)$ for all r at $t = 0.1$. The initial clustering is accidentally stronger for positive PVs than the negative. This fact can be regarded as clustering to a single vortex at the largest scale. There is also a significant void where positive (or negative) PVs do not exist at $t = t_f$. We can also consider the initial *fractal* distribution like Sierpinski's Gasket which shows clustering at large scales.

Finally we consider the CSR distributions of two kinds of PV, Case (VII). A remarkable feature in this turbulent situation is that there are several pairs of a positive and negative vortex moving linearly at a velocity $\kappa/4h\pi$, where $2h$ is a distance of two PVs. Since the pair is surrounded by a number of other isolated PVs, however, the moving direction is bent by a third vortex when they pass each other. Moreover, if the collision is nearly head-on, a vortex of the pair with the opposite sign of the third target vortex replaces its partner by the latter and then continues to move linearly again. An exact analysis of such scattering of three PVs in an unbounded domain was already given by Aref (1979).⁸

Examples of scattering and recoupling of three PVs in a periodic box are given by an initial location $(z_1, z_2, z_3) = (L + iL, (L + d + h)i, (L + d - h)i)$ with $L = 1/2$. A pair of vortex 2 and 3 is approaching vortex 1 initially. Figure 4a shows their trajectories in the cases $h = 0.02$ and $d = \pm 0.02, \pm 0.01, 0.04, 0.08, 0.16$ and 0.32 . The final time t_f is 0.04 except for $t_f = 0.1$ for $d = 0.16$, $t_f = 0.05$ for $d = 0.32$ and $t_f = 0.06$ for $d = -0.01$. Recoupling is observed for $d = 0.01, 0.02, 0.04, 0.08$ and 0.16 . The dependence of a π -normalized scattering angle $\delta\phi/\pi$ measured by the moving direction of $z_3(t = 0.04)$ for $h = 0.02$ in a periodic box is shown in Figure 4b. The recoupling of PVs in an unbounded plane with $L \rightarrow \infty$ ⁸ occurs if $0 < d/h < 9$. On the other hand, the present simulation in a periodic box with $h = 0.02$ shows a shift of the range d for recoupling as $-0.5 \lesssim d/h \lesssim 8.5$, although this range may vary as h is changed in the case of periodic BCs. In a GIF animation, successive scattering and recoupling, similar to chaos in the billiard system, are clearly observed. An existence of such vortex pairs may play a crucial role of stirring assemblies of PVs.

Since an average distance of randomly located PVs is $l \sim N^{-1/2}$ and the strength is fixed 2π , a typical velocity and eddy turnover time is respectively $v \sim N^{1/2}$ and $t_e \sim 1/N$. Denoting the smallest distance of the vortex pair by αl , its velocity is $V \sim 1/\alpha l$. Because of the recoupling condition, the cross section of the scattering is about $\sigma_c \sim d \sim 10\alpha l$ and the area swept by the pair during t_e is $S \sim dVt_e \sim 10/N$. Therefore the condition for the scattering to occur in t_e is $N \sim 10$ since $S \sim 1$, the size of the square. If $N = 100$, $t_e \sim 0.01$ and approximately one pair will be scattered ten times in a numerical simulation in the time interval $0 \leq t \leq 0.1 \sim 10t_e$.

The $L_{lm}(r)$ function becomes slightly positive for $(l, m) = (+, -)$, which also indicates that the pairs of positive and negative PVs survive until $t = 0.1$. But the

absolute values are much smaller than the initially clustered cases. To see the spontaneous clustering clearly, longer simulations may be required. We also investi-

Table I. The cases of a single kind of PVs

Case	N	t_f	H	I_x	I_y
I	100	0.01	17948	50.5	0
II	96	0.1	11973	47.872	47.923
III	100	0.1	12796	49.968	50.020
IV	100	0.1	12886	49.687	50.206

Table II. The cases of two kinds of PVs

Case	$N_{1,2}$	t_f	H	I_x	I_y
V	50	0.01	-415.31	-0.50019	-0.49976
VI	48	0.1	369.60	-12.176	-11.081
VII	50	0.1	-178.31	-1.9433	2.3455

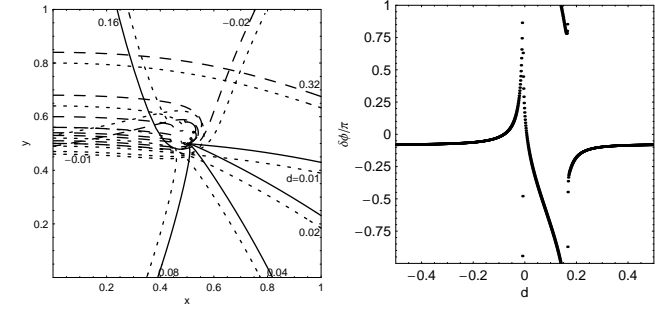


Fig. 4. (a) Trajectories of three scattering and recoupling PVs for various values of h . Solid, dashed and dotted curves denote z_1 , z_2 and z_3 respectively. (b) The π -normalized scattering angle $\delta\phi/\pi$ versus d for $h = 0.02$.

gated the PDF of velocity circulation, which is studied in Umeki (1993)⁹ in three-dimensional turbulence.¹⁰ A similar approach in point process theory is called the Quadrat method.⁵

In summary, a method to simulate motions of PVs with periodic BCs using *Mathematica* is described. Several numerical examples are shown and clustering of PVs with different conditions is examined by the L function.

The author is grateful to Professor Yamagata for support of his research on fluid dynamics during these several years.

- 1) V. K. Tkachenko, *Sov. Phys. J.E.T.P.* **22** (1966) 1282.
- 2) V. K. Tkachenko, *Sov. Phys. J.E.T.P.* **23** (1966) 1049.
- 3) M. A. Stremler and H. Aref, *J. Fluid Mech.* **392** (1999) 101.
- 4) P. G. Saffman, *Vortex Dynamics* (Cambridge University Press) (1992).
- 5) N. A. C. Cressie, *Statistics for Spatial Data, Revised Edition* (1993).
- 6) K. Shimatani, *Jpn. J. Ecology* **51** (2001) 87 (in Japanese).
- 7) E. A. Novikov, *Sov. Phys. JETP* **41** (1976) 937.
- 8) H. Aref, *Phys. Fluids* **22** (1979) 393.
- 9) M. Umeki, *J. Phys. Soc. Jpn.* **62** (1993) 3788.
- 10) A. A. Migdal, *Int. J. Mod. Phys.* **A10** (1994) 1197.